Eur. Phys. J. B **55**, 13–22 (2007)
DOI: 10.1140/epjb/e2007-00031-9

THE EUROPEAN PHYSICAL JOURNAL B

Quantum size effects on the (0001) surface of double hexagonal close packed americium

D. Gao[a] and A.K. Ray[b]

Physics Department, P.O. Box 19059, University of Texas at Arlington, Arlington, Texas 76019, USA

Received 2 October 2006 / Received in final form 10 January 2007
Published online 2 February 2007 –

Abstract. Electronic structures of double hexagonal close-packed americium and the (0001) surface have been studied via full-potential all-electron density-functional calculations with a mixed APW+lo/LAPW basis. The electronic and geometric properties of bulk dhcp Am as well as quantum size effects in the surface energies and the work functions of the dhcp Am (0001) ultra thin films up to seven layers have been examined at nonmagnetic, ferromagnetic, and antiferromagnetic configurations with and without spin orbit coupling. The anti-ferromagnetic state including spin-orbit coupling is found to be the ground state of dhcp Am with the $5f$ electrons primarily localized. Our results show that both magnetic configurations and spin-orbit coupling play important roles in determining the equilibrium lattice constant, the bulk modulus as well as the localized feature of $5f$ electrons for dhcp Am. Our calculated equilibrium lattice constant and bulk modulus at the ground state are in good agreement with the experimental values respectively. The work function of dhcp Am (0001) 7-layer surface at the ground state is predicted to be 2.90 eV. The surface energy for dhcp Am (0001) semi-infinite surface energy at the ground state is predicted to be 0.84 J/m^2. Quantum size effects are found to be more pronounced in work functions than in surface energies.

PACS. 71.15.-m Methods of electronic structure calculations – 71.27.+a Strongly correlated electron systems; heavy fermions – 73.20.At Surface states, band structure, electron density of states – 75.50.Ee Antiferromagnetics

1 Introduction

Considerable experimental and theoretical efforts have been devoted to studying the electronic and geometric structures and related properties of surfaces to high accuracy in recent years. Actinides, as a group of strongly correlated and heavy fermion systems, especially have received notable increasing interests [1–5]. As is known, experimental work on actinides is relatively difficult to perform due to material problems and toxicity. On the other hand, they play important roles in advanced nuclear fuel cycles. Hence, theoretical studies are crucial for these high-Z elements. Such studies may also lead to a better understanding of the detailed surface corrosion mechanisms in the presence of environmental gases and thus help to address the environmental consequences of nuclear materials.

Among the actinides, the unique electronic properties of americium (Am), which was first successfully synthesized and isolated at the wartime Metallurgical Laboratory [6], have received increased interests recently, from both scientific and technological points of view. It has been noted that Am occupies a pivotal position in the actinide series with regard to the behavior of $5f$ electrons [7]. Atomic volumes of the actinides as a function of atomic number have experimentally displayed a sharp increase between Pu and Am [8]. In contrast to this sharp increase, the atomic volumes of the actinides before Pu continuously decreases as a function of increasing atomic number from Ac until Np, which is analogous to d transition metals. These behaviors reveal that the properties of the $5f$ electrons change dramatically starting from somewhere between Pu and Am. It has been suggested [9,10] that the $5f$ electrons of the actinides before Am (until Pu) participate in bonding while the $5f$ electrons of the actinides after Pu (starting from Am) become localized and non bonding. Both theoretical calculations [11] and the X-ray and high-resolution ultraviolet photoemission study [12] of the $5f$ electrons in Am have supported the localized picture for Am. Another notable feature is the high-pressure behavior of americium. As pressure increases, the crystal structures of americium display the following phase transitions [13]: double hexagonal close packed

[a] *Present address*: Center for Advanced Modeling and Simulation, Idaho National Laboratory, Idaho Falls, ID 83415, USA.
[b] e-mail: akr@uta.edu

(Am I) → face-centered cubic (Am II) → face-centered orthorhombic (Am III) → primitive orthorhombic (Am IV). Although experimental data indicates that the phase transition from Am II to Am III is probably accompanied with the $5f$ electron delocalization [7,13], recent density-functional studies by Penicaud [14] regarding the high-pressure behavior of americium found that only the fourth phase (Am IV) is delocalized and the $5f$ electrons of the three previous americium phases are localized. The dynamical mean field theory calculations by Savrasov et al. [15] also indicate that the location of the Mott transition is near the Am III to Am IV boundary and that the f electrons start to participate in bonding in the highly pressurized Am IV structure. Using the full-potential linear muffin-tin orbital (FP-LMTO) method, Sõderlind et al. [16] calculated the total energies of fcc, bcc, bcm (α''), α-U(α'), α-Np, and α-Pu structures of Am as a function of volume. At 80 kbar, they calculated a transition from fcc Am to monoclinic Am and a volume collapse of 25%. They interpreted this as a Mott transition and the onset of a low symmetry crystal structure was induced by $5f$ electron delocalization in Am. A later study by Sõderlind and Landa [16] indicated that the Am I phase was stabilized by contributions from the d shell to the cohesion whereas all other phases follow from $5f$ electron bonding i.e. delocalization. Such controversies clearly indicate that further experimental and theoretical studies are needed to improve our understanding of americium and the associated $5f$ electrons.

Another controversy surrounding Am is the question of magnetism. Experimental results, in general, indicate that Am is nonmagnetic. For example, Naegele et al. [12], in their photoemission study of the localization of $5f$ electrons in Am, assumed the ground-state electron configuration to be $5f^6$ (nonmagnetic). Huray et al. [17] in their experimental studies of the magnetism of the heavy $5f$ elements also found Am to have zero effective magnetic moment with an f^6 probable ion configuration. Both Gouder et al. and Cox et al. [18], in their respective photoemission studies, found Am to have localized f states in a $5f^6$ configuration, consistent with the absence of magnetic order. On the other hand, theoretical studies on Am metal, mostly based on ab initio self-consistent density functional theory, in general, indicate the presence of magnetism [14,16,19–21]. Using fully relativistic, full-potential linear-muffin-tin-orbital calculations, Eriksson and Wills [20] reported strong disagreements with experimental data. Using the same method as also canonical band theory, Soderlind and Landa [16] actually found the fcc phase to be stable by a small margin over dhcp but when d contribution is included, their energies were degenerate. They also found that the $5f$ electrons in Am almost entirely spin-polarize. Penicaud [14] modeled the localization of the $5f$ electrons by an anti-ferromagnetic (AFM) configuration found to have a lower energy than a ferromagnetic configuration. Using the full potential Dirac relativistic basis, spin-polarized linearized-augmented-plane-wave method, Kutepov and Kutepova [21] found also the AFM ordering to be favored for dhcp Am. The around-men-field LSDA+U (AMF-LSDA+U) correlated band theory has been applied by Shick et al. [22] to study the electronic and magnetic structure of fcc-Pu-Am alloys. For fcc Am, they performed AMF-LSDA+U calculations, varying the Coulomb U from 3 eV to 4 eV and keeping the inter-atomic exchange parameter J at 0.75 eV. The calculations yielded practically zero magnetic moment, with an equilibrium atomic volume of 186 (a.u.)^3 and a bulk modulus of 55.1 GPa with $U = 4$ eV. Kotliar et al. [23] have used dynamical-mean-field-theory (DMFT) approach to study strongly correlated systems, such as the actinides. Using a DMFT-based spectral density functional approach, they observed that the f electrons in Am at zero pressure exists in a $f^6\ {}^7F_0$ configuration, with a U value of about 4.5 eV. Our calculations for fcc Am II [19], using the FP-LAPW method, yielded an AFM state, with an equilibrium atomic volume of 195.3 (a.u.)^3 and a bulk modulus of 28.1 GPa. The experimental equilibrium volume is 198.5 (a.u.)^3 and a bulk modulus of 29.4 GPa. On the other hand, results at the NSP-SO level produce an equilibrium atomic volume of 137.8 (a.u.)^3 and a bulk modulus of 63.8 GPa. Thus, a non-magnetic calculation produces an error of 31% in the atomic volume and 117% in the bulk modulus! Savrasov et al. [15] have found that a nonmagnetic GGA calculation failed catastrophically in reproducing the equilibrium volume of the soft phase of Am by about 50%. Clearly, there is strong disagreement here between theory and experiment as far as the question of magnetism is concerned. Given this wide spectrum of results on Am, we believe that a systematic and fully relativistic density functional study of Pu and Am surface chemistry and physics using the same level of theory could certainly lead to significant insights and knowledge about the actinides and at the very least, produce a qualitative and quantitative trend in our understanding of the light to heavy actinides and stimulate further work in actinides.

The electronic structure of americium, wherein six f electrons presumably form an inert core, decoupled from the *spd* electrons that control the physical properties of the material, also contributes to the superconductivity in Am [24,25]. Recently, a study of the superconductivity in americium [26] as a function of pressure has showed that such studies may be an effective method to understand the unique $5f$ electron properties of americium including the Mott transition, i.e., the evolution of the $5f$ electrons from localized to the delocalized.

Another effective way to probe the actinides (including americium) $5f$ electron properties and their roles in chemical bonding is the study of their surface properties. The unusual aspects of the bonding in bulk Am are apt to be enhanced at a surface or in a thin layer of Am adsorbed on a substrate, as a result of the reduced atomic coordination of a surface atom and the narrow bandwidth of surface states. Thus, Am surfaces and thin films may also provide valuable information about the bonding in Am. However, to the best of our knowledge, *very few* studies exist in the literature about the Am surface, especially surfaces of the double hexagonal close packed (dhcp) structure Am (Am I), which is the most common phase of Am under normal pressure.

We have recently reported the bulk and surface properties of fcc δ-Pu and atomic and molecular adsorptions on such surfaces and also bulk and (111) and (001) surfaces of fcc Am II [19,27]. As a continuation of our systematic and fully relativistic density functional studies of actinide surface physics and chemistry, in this work, we report, in *some* detail the electronic structure properties of dhcp Am I bulk and the (0001) surface and compare them with the corresponding properties of fcc Am II. Other motivations for such a study also stem from the following observations: (1) both plutonium and americium represent the boundary between the "light" actinides, Th to Pu, and the "heavy" actinides, Am and beyond; (2) whereas, Pu has an open shell of f electrons, Am is closer to a full $j = 5/2$ shell; (3) the transition from delocalization-to-localization supposedly takes place somewhere between Pu and Am; yet there is no such apparent transition observed, at least, in α-Pu although the $5f$ electrons of δ-Pu are partially localized [1–10,15,23,27], as indicated by its atomic volume, which is approximately halfway between α-Pu and Am. For such studies, it is common practice to model the surface of a semi-infinite solid with an ultra thin film (UTF), which is thin enough to be treated with high-precision density-functional calculations, but is thick enough to realistically model the semi-infinite surface. Determination of an appropriate UTF thickness is complicated by the existence of possible quantum oscillations in UTF properties as a function of thickness, the so-called quantum size effect (QSE). These oscillations were first predicted by calculations on jellium films [28,29] and were subsequently confirmed by band-structure calculations on free-standing UTFs composed of discrete atoms [30–33]. The adequacy of the UTF approximation obviously depends on the size of any QSE in the relevant properties of the model film. Thus, it is important to determine the magnitude of the QSE in a given UTF prior to using that UTF as a model for the surface. This is particularly important for Am films, since the strength of the QSE is expected to increase with the number of valence electrons [28]. Though the purpose of this work is to study the properties of Am I (0001) surface, specifically, the quantum size effects, we have first optimized bulk Am I. Due to severe demands on computational resources and internal consistency, we have not considered the possibilities of surface relaxations and reconstructions; instead, the equilibrium bulk lattice constants obtained at each level of theory have been used to build the (0001) surface slabs with one atom per layer up to seven layers. We do not believe that this approximation will, in any way, alter the primary qualitative and quantitative conclusions of this study. We should note also that any relaxation is expected to be quite small. In fact, we carried out *preliminary* relaxation studies of a 3-layer Am film. The separation distance between the first and second layer increased by 2.1% and that between the second and third layer decreased by 0.9%, with the total energy difference between the relaxed and unrelaxed surfaces being 8.39 meV/atom. Thus the effects on physical quantities of interest in this work such as spin-polarization energies, spin-orbit coupling energies, surface energies, and work functions are expected to be insignificant. We first discuss briefly the computational method, followed by results and discussions.

2 Computational method

The present computations have been carried out using the full-potential all-electron method with mixed basis APW+lo/LAPW method implemented in the WIEN2k software [34–36]. The generalized-gradient-approximation (GGA) with a gradient corrected Perdew-Berke-Ernzerhof (PBE) exchange-correlation functional [37] to density functional theory [38] is used and the Brillouin-zone integrations are conducted by an improved tetrahedron method of Blöchl-Jepsen-Andersen [39]. In the WIEN2k code, the alternative basis set APW+lo is used inside the atomic spheres for the chemically important orbitals that are difficult to converge, whereas LAPW is used for others. The local orbitals scheme leads to significantly smaller basis sets and the corresponding reductions in computing time, given that the overall scaling of LAPW and APW + lo is given by N^3, where N is the number of atoms. Also, results obtained with the APW + lo basis set converge much faster and often more systematically towards the final value [40]. To model the AFM state, alternative layers of the thin film are occupied by up and down spins along the c-axis. As far as relativistic effects are concerned, core states are treated fully relativistically in WIEN2k and for valence states, two levels of treatments are implemented: (1) a scalar relativistic scheme that describes the main contraction or expansion of various orbitals due to the mass-velocity correction and the Darwin s-shift [41] and (2) a fully relativistic scheme with spin-orbit coupling included in a second variational treatment using the scalar-relativistic eigenfunctions as basis [42,43]. The present computations have been carried out at both scalar-relativistic and fully-relativistic levels to determine the effects of relativity. To calculate the total energy, a constant muffin-tin radius (R_{mt}) of 2.60 a.u. is used and the plane-wave cut-off K_{cut} is determined by $R_{mt}\ K_{cut} = 9.0$ for all calculations. The Brillouin zone is sampled on a uniform mesh with 111 irreducible K-points for the bulk calculations. The (0001) surface of dhcp Am is modeled by periodically repeated slabs of N Am layers (with one atom per layer and $N = 1$–7) separated by an 80 a.u. vacuum gap. Twenty-one irreducible K points have been used for reciprocal-space integrations. For each calculation, the energy convergence criterion is set to be 0.01 mRy. We first discuss below the results for bulk dhcp Am, followed by detailed results for the (0001) surface of dhcp Am.

3 Results and discussions

3.1 Bulk properties

Bulk Am I has a dhcp crystal structure [44] with four atoms per unit cell, two in positions $2a$ (0 0 0; 0 0 1/2) and two in positions $2d$ (1/3 2/3 3/4; 2/3 1/3 1/4). With

Table 1. Calculated physical properties of dhcp Am bulk.

Method	a (a.u.)	c (a.u.)	Atomic volume (a.u.^{3})	Bulk modulus (GPa)	Total energy differences (Ry/atom)
NM-NSO[a]	5.54	17.73	117.81	159.80[b], 156.40[c]	0.750388
NM-SO[a]	5.82	18.62	136.55	68.07[b], 70.82[c]	0.111926
FM-NSO[a]	6.92	22.14	229.54	23.71[b], 23.82[c]	0.567889
FM-SO[a]	6.82	21.82	219.73	25.06[b], 25.11[c]	0.003028
AFM-NSO[a]	6.73	21.54	211.23	20.98[b], 20.96[c]	0.568108
AFM-SO[a]	6.61	21.15	200.07	26.97[b], 27.08[c]	0.0
RSPFLAPW (NM)[d]	N/A	N/A	134.4	70.0	
RSPFLAPW (AFM)[d]	N/A	N/A	197.3	28.3	
MTO (FPLAPW) [e]	N/A	N/A	201.45	46.8	
Experimental	6.56[f]	21.26[f]	198.38[g]	29.9[h], 45[i]	

[a] The present work; [b] EOS values; [c] EOS2 values; [d] reference [21]; [e] reference [14]; [f] reference [44]; [g] reference [14]; [h] reference [13]; [i] reference [51].

the experimental value of ideal c/a ratio [44], we first calculated the total energies for a set of different lattice constants a at six different theoretical levels i.e., AFM-SO, AFM-NSO, FM-SO, FM-NSO, NM-SO, and NM-NSO. Around the minimum energy several more points with a lattice constant difference of 0.01 a.u. have been searched again to locate the optimized equilibrium lattice constant. To obtain the bulk modulus, we used both the Murnaghan equation of state (EOS) [45]

$$E = BV/\beta[1/(\beta-1)(V_0/V)^{\beta}+1], \quad (1)$$

and EOS2 [46]

$$E = a + bV^{-1/3} + cV^{-2/3} + dV^{-1}, \quad (2)$$

to fit the total energy vs. volume curve through a volume optimization tool available in WIEN2K. Results are listed in Table 1 and compared to *some* of the available theoretical and experimental results. Our results show that, at the nonmagnetic state, the equilibrium lattice constant a of dhcp Am is underestimated by 11% and 16%, with and without SO coupling, respectively, compared to the experimental value. Compared to the experimental value, the bulk modulus is significantly overestimated with both EOS and EOS2 at the NM-SO and NM-NSO levels. At the ferromagnetic configuration, the values of both equilibrium lattice constant a and the bulk modulus are substantially improved as compared with the experimental values of these quantities. To be specific, the equilibrium lattice constant a of dhcp Am now is overestimated by 4% and 5%, with and without SO coupling, respectively, compared to the experimental value. For the bulk modulus, it is underestimated by about 16% and 21% with both EOS and EOS2 at the FM-SO and FM-NSO level, respectively, compared to the experimental value from reference [13]. In the anti-ferromagnetic configuration, especially with spin orbit coupling included, both the equilibrium lattice constant a and the bulk modulus obtained from our calculations are in very good agreement with the experimental values. The equilibrium lattice constant a of dhcp Am obtained at the AFM-SO and AFM-NSO level is overestimated by 0.8% and 2.6%, respectively, compared to the experimental value. At the AFM-SO level, the bulk modulus obtained is also significantly improved compared to the experimental bulk modulus value from reference [13] with both EOS2 and EOS. From Table 1 we can see the underestimation is about 9% with EOS2 and 10% with EOS compared to the experimental bulk modulus from reference [13]. Our total energy results also clearly indicate that the ground state of dhcp Am is antiferromagnetic with spin orbit coupling, in agreement with other first-principles studies [14,16,21]. It is worth noting that, without the inclusion of spin-orbit coupling, the AFM-NSO and FM-NSO levels are practically degenerate, with the FM-NSO level being actually very slightly lower, 0.000219 Ry/atom, in energy. With the inclusion of spin-orbit coupling, the degeneracy is slightly lifted, with the AFM-SO now being lower in energy, by 0.003028 Ry/atom compared to FM-SO state. We also wish to stress here, that without spin-polarization and spin-orbit coupling, DFT simply fails to reproduce theoretical values close to the experimental values for the equilibrium lattice constant and bulk modulus, as in Am I mentioned before. Also, the bulk modulus obtained via EOS2 is closer to the experimental bulk modulus compared to the value obtained via EOS, especially at the AFM-SO level, although the improvement is not very significant.

Similar to the AFM-SO ground state nature of dhcp Am bulk, our previous calculations for fcc Am II have also indicated an AFM-SO ground state [19]. Moreover, our results indicate that Am I has a lower total energy than Am II, though it is very small about 0.1 mRy/atom. On the contrary, a recent FPLMTO study [16] showed that Am II has a lower total energy than Am I with around 0.1 mRy/atom difference. Thus, both studies support the notion that the total energy difference between Am I and Am II is negligible and the two phases Am I and Am II are basically degenerate theoretically. Thus, no reliable transition pressure between these two phases can be determined from the current electronic structure studies.

We also calculated the spin-orbit coupling energy E_{so} defined by

$$E_{so} = E_{tot}(NSO) - E_{tot}(SO), \tag{3}$$

at the equilibrium lattice constant to further assess the effects brought by SO. The spin-orbit coupling energy E_{so} obtained at the NM, FM and AFM level is 8.69 eV, 7.69 eV, and 7.73 eV respectively. In general, the SO coupling effect is notable and will lower the total energy, although the LAPW method avoids the well-known variational collapse problem because of the way the basis set is formed, and the second-variational treatment is expected to slightly underestimate the effects of spin-orbit coupling. On the other hand, spin-polarization energy, defined at the difference in total energies at the SP and NSP levels of theory, with and without SO coupling included, are calculated to be 2.48 eV/atom, 1.48 eV/atom, 2.48 eV/atom, and 1.52 eV/atom, at the FM-NSO level, FM-SO, AFM-NSO, and AFM-SO levels, respectively. Thus, spin-orbit coupling energies are significantly larger than spin-polarization energies at all levels of theory, underscoring the importance of spin-orbit coupling compared to spin-polarization.

3.2 (0001) surface properties

Since experimental results indicate a non-magnetic nature for Am I and theoretical calculations indicate an AFM configuration, for the surface studies, we have carried out calculations at the AFM-SO, AFM-NSO, NM-SO, and NM-NSO theoretical levels to not only study quantum size effects but also to determine the effects of spin and relativity for the Am I surface. Another reason for considering the non-magnetic state is because experimentally Am is supposed to be non-magnetic. Calculations of the total energy for dhcp Am (0001) films at different theoretical levels indicate that the ground state is AFM-SO, in agreement with the results for dhcp Am bulk. The cohesive energies E_{coh} for the dhcp Am (0001) N-layer slabs have been calculated from the difference between the total energy per atom of the monolayer and the total energy per atom of the N-layer slab and are found to increase monotonously with the slab thickness (shown in Fig. 1) at all four levels of theories. It is also noticeable that the rate of increase of cohesive energy drops significantly as the number of layers increase, and it is expected that the convergence in the cohesive energy can be achieved after a few more layers. However, since to the best of our knowledge, the experimental value for the semi-infinite surface cohesive energy is not known, we are unable to predict how many layers will be needed to achieve the semi-infinite surface energy. Typically, antiferromagnetic state significantly lowers the cohesive energy at both the scalar relativistic and fully relativistic levels of theory. On the other hand, spin-orbit coupling increases the cohesive energy by about ∼7–10% at both nonmagnetic and antiferromagnetic states. All cohesive energies are positive, indicating that all layers of dhcp Am (0001) films are bound relative to the monolayer.

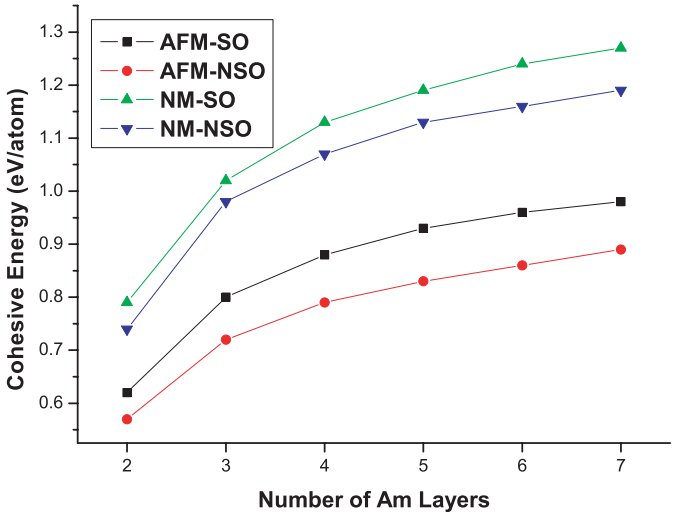

Fig. 1. Cohesive energies per atom of the dhcp Am (0001) films with respect to the Am monolayer versus the number of Am layers.

As is known, the two primary quantities of interest for quantum size effects are the surface energy and the work function. The surface energy for a N-layer dhcp Am (0001) film has been estimated from [47]

$$E_s = (1/2)[E_{tot}(N) - NE_B], \tag{4}$$

where $E_{tot}(N)$ is the total energy of the N-layer slab and E_B is the total energy per atom of the bulk crystal. Since we have used one atom per layer, N-layer film has N atoms. If N is sufficiently large and $E_{tot}(N)$ and E_B are known to infinite precision, equation (4) is exact. If, however, the bulk and film calculations are not entirely consistent with each other, E_s will diverge linearly with increasing N. Stable and internally consistent estimates of E_s and E_B can, however, be extracted from a series of values of $E_{tot}(N)$ via a linear least-squares fit to [48]

$$E_{tot}(N) = E_B N + 2E_s. \tag{5}$$

To obtain an optimal result, the fit to equation (5) should only be applied to films which include, at least, one bulk-like layer, i.e., $N > 2$. We have independently applied this fitting procedure to the dhcp Am (0001) films at all four levels of theory, respectively. Accordingly, four values of E_B, i.e., –61041.709845, –61042.351641, –61041.891373, and –61042.461052 Ry are derived for the dhcp Am (0001) films at the NM-NSO, NM-SO, AFM-NSO, and AFM-SO levels, respectively. Compared to these derived values, the previously obtained total energies at the NM-NSO, NM-SO, AFM-NSO, and AFM-SO levels are –61041.708447, –61042.346909, –61041.890727, and –61042.458835 Ry, respectively. Thus the derived E_B values, at the four levels of theory, are 1,4, 4.7, 0.6, 2.2 mRy lower in energy, respectively. This is attributed to the finite number of slabs used in this study. The surface energy for each film has been computed using the calculated N-layer total energy and appropriate fitted bulk energy. The results are plotted in Figure 2. For all surface energies several features

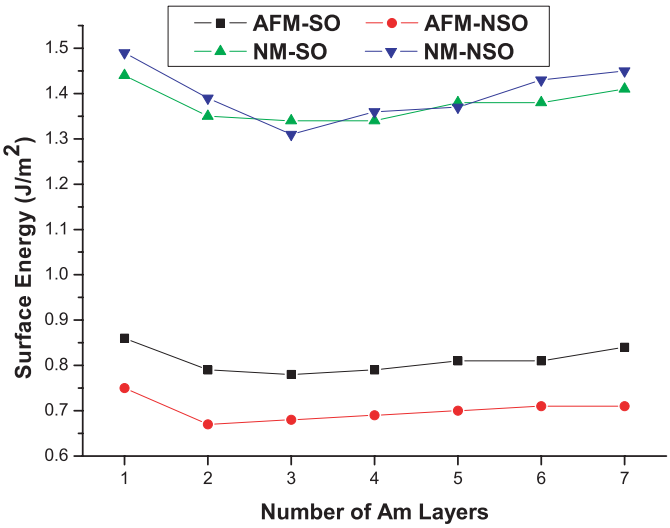

Fig. 2. Surface energies for the dhcp Am (0001) films vs. the number of Am layers.

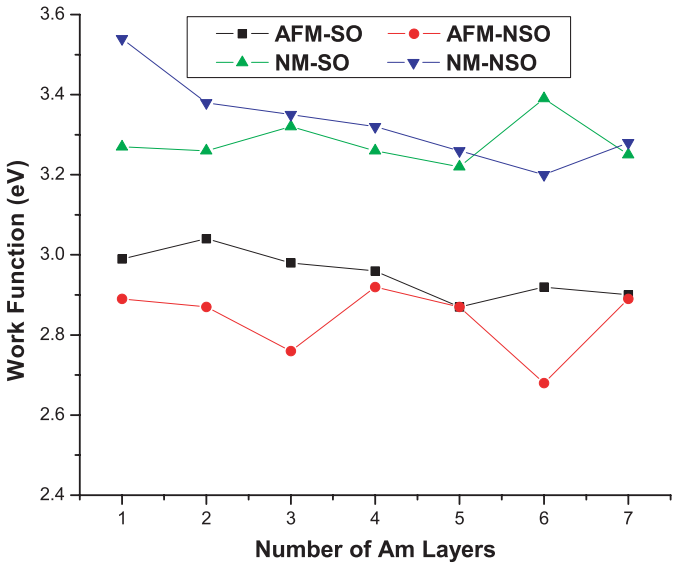

Fig. 3. Work functions (eV) of the dhcp Am (0001) films vs. the number of Am layers.

are evident from our results. First, surface energy values tend to saturate when the number of layers reaches three at both AFM-NSO and AFM-SO levels; however, this is not the case for NM-NSO and NM-SO levels. Specifically, the fluctuations from layers 3 to 7 for the NM cases are more than those at the AFM cases. For example, at the NM-NSO level, the deviation (the maximum difference between two values divided by the maximum value) is 10%, while at the AFM-SO level, the difference only 4%. From these results, we again infer that a surface model with a three layer film may be sufficient for future atomic and molecular adsorption studies on Am films, if the primary quantity of interest is the chemisorption energy. This is similar to our previous study of fcc Pu and Am surfaces, where also we found that a three layer film is adequate for chemisorption studies [19,27]. Second, compared to spin orbit coupling, the antiferromagnetic state plays a more significant effect on surface energy. To be specific, for dhcp Am (0001) films, the antiferromagnetic state lowers the surface energy from ∼1.4 J/m^2 to ∼0.8 J/m^2. Third, the surface energy of dhcp Am (0001) seven layers film at the ground state, i.e., at the AFM-SO level, is calculated to be 0.84 J/m^2 and we believe that this is also a fairly good estimate of the semi-infinite (0001) surface energy. We hasten to point out that though we have used the method discussed in reference [48] to evaluate surface energies, several methods of calculating convergent surface energies from slab calculations has been critically compared by Fiorentini and Methfesel [49].

We have also studied the dependence of the work function on the dhcp Am (0001) layer thickness. The work function, W, is calculated according to the following formula

$$W = V_0 - E_F, \tag{6}$$

where V_0 is the Coulomb potential energy at the half height of the slab including the vacuum layer and E_F is the Fermi energy. As mentioned before, an 80 a.u. vacuum gap was used in the calculations. This is a rather large gap but was deemed to be necessary for convergence in the quantities used in equation (6). As mentioned by Fall et al. [50], QSE can influence accurate determinations of WFs from thin slab calculations. The work functions of dhcp Am (0001) films up to seven layers have been calculated at the four theoretical levels, i.e., NM-NSO, NM-SO, AFM-NSO, and AFM-SO, respectively, and the results are plotted in Figure 3. We note that the work functions show some oscillations at all four theoretical levels up to seven layers. From the current results, we can infer that at least a 7-layer film may be required for any future adsorption investigation that requires, for example, an *accurate* prediction of one-electron properties and adsorbate-induced work function shift. On the other hand, a strong QSE was observed for both fcc Am (110) and (001) films up to seven layers while the work function for fcc Am (111) films becomes relatively stable as the number of layers reaches five [19]. For fcc δ-Pu, the number of layers for stabilizations of the work functions are 5, 5 and 7, for (111), (001), and (110), respectively. The calculated work functions of dhcp Am 7-layers (0001) film are found to be 3.28, 3.25, 2.89, and 2.90 eV at the NM-NSO, NM-SO, AFM-NSO, and AFM-SO levels, respectively. These values showed that work functions are obviously lowered when the antiferromagnetic configuration is introduced. However, the spin orbit coupling effect on work function is small and may be negligible as the number of layers increase. We note that though, at the AFM level, for layers 3–7 (except for 6) the AFM-NSO and AFM-SO WF values are rather close to each other. We do not believe that there is any particular physical reason for this; however, a systematic study with large number of layers (certainly significantly larger than 7) may be necessary to determine that dependence of WF on SO coupling effects. We note that at the ground state, the work functions for fcc Am (110), (001), and (111) films with 7-layers have been calculated to be 2.86, 2.93, and 3.06 eV, respectively and for δ-Pu, the

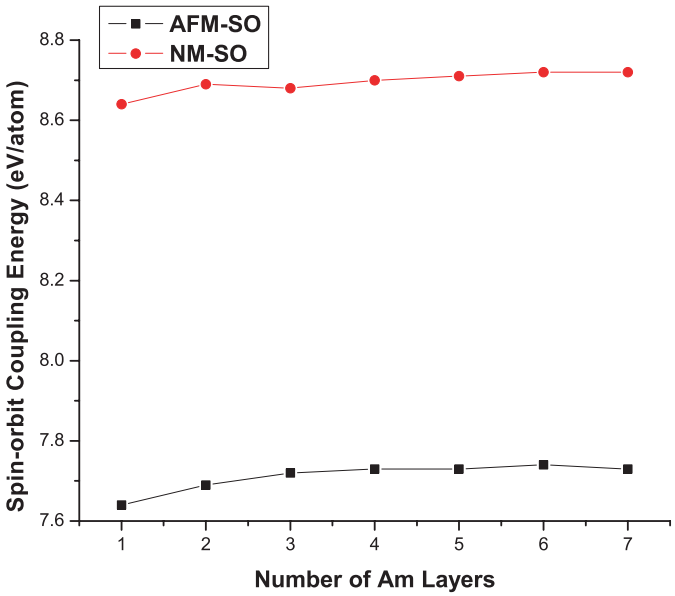

Fig. 4. Spin-orbit coupling energies (eV/atom) for dhcp Am (0001) films for N layers ($N = 1$–7).

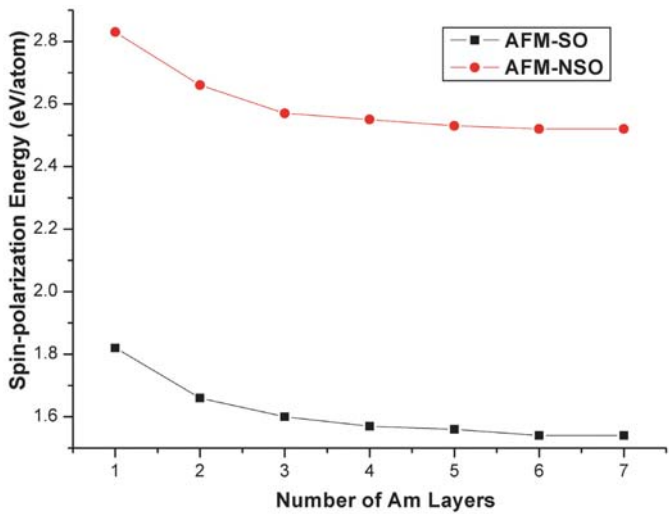

Fig. 5. Spin-polarization energies (eV/atom) for dhcp Am (0001) films with N layers ($N = 1$–7).

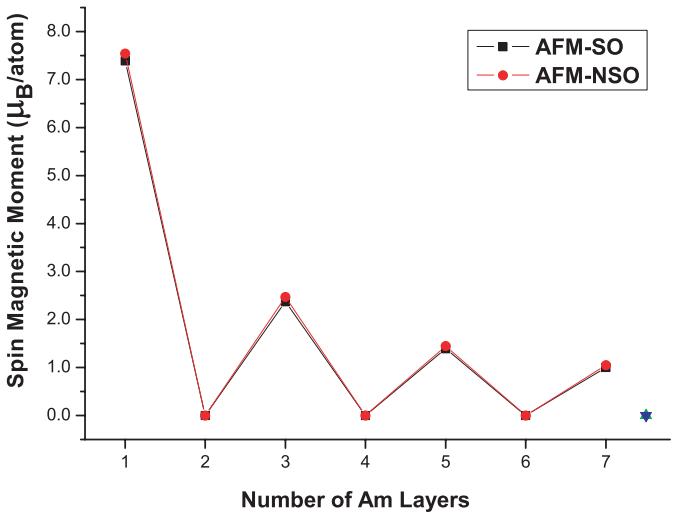

Fig. 6. Spin magnetic moments of the dhcp Am (0001) films for different layers ($N = 1$–7). The corresponding spin magnetic moments of the dhcp Am bulk are also shown at the right of the figure.

corresponding values are 2.99, 3.11, and 3.41 eV at the same level of theory [19,27].

The spin-orbit coupling energy E_{so}, defined for the surface as for the bulk in equation (3), for the dhcp Am (0001) films at both nonmagnetic and antiferromagnetic levels have been calculated up to seven layers, and the results are plotted in Figure 4. It is found that the spin orbit coupling energies become rather stable when the number of layers equals three. It can also be seen that spin-orbit coupling plays an important role in reducing the total energies of the dhcp Am (0001) films, i.e., spin-orbit coupling effect reduces the total energy by ∼8.7 eV/atom at the nonmagnetic state and ∼7.7 eV/atom at the antiferromagnetic state.

We also calculated the spin-polarization energy E_{sp} defined by

$$E_{SP} = E_{tot}(NSP) - E_{tot}(SP). \quad (7)$$

The results are plotted in Figure 5. We note that at both levels, spin-polarization energy decreases as the number of layers increases, reaching saturation at six layers. Spin-polarization energy at the NSO level is consistently higher than the corresponding values at the SO level, indicating, among others, the importance of spin-orbit coupling. The converged spin-polarization energies are 2.52 eV/atom and 1.54 eV/atom at the NSO and SO levels, respectively.

The spin magnetic moments of dhcp Am (0001) films per atom at the AFM-NSO, and AFM-SO levels, have also been calculated. In Figure 6, we have plotted the moments for dhcp Am (0001) films as well as the corresponding values for dhcp Am bulk. Several features have been observed. First, for the dhcp Am (0001) films at both AFM-NSO and AFM-SO levels, the magnetic moments show a behavior of oscillation, which becomes smaller with the increase of the number of layers, and gradually the magnetic moments approach the bulk value of zero. The dhcp Am (0001) films with an odd number of layers have magnetic moments decreasing with the increase of the number of layers, while the dhcp Am (0001) films with an even number of layers always have zero magnetic moments same as that of dhcp Am bulk. To some extent, this is an artifact of the surface model used. We believe that the important thing to note here, as mentioned above, is that the magnetic moments of the films with odd numbers of layers gradually decrease. Second, for the dhcp Am (0001) films at the anti-ferromagnetic state, the spin-orbit coupling has negligible effect on the magnetic properties. These features have been previously observed in the magnetic properties of fcc Am and δ-Pu films as well [19,27].

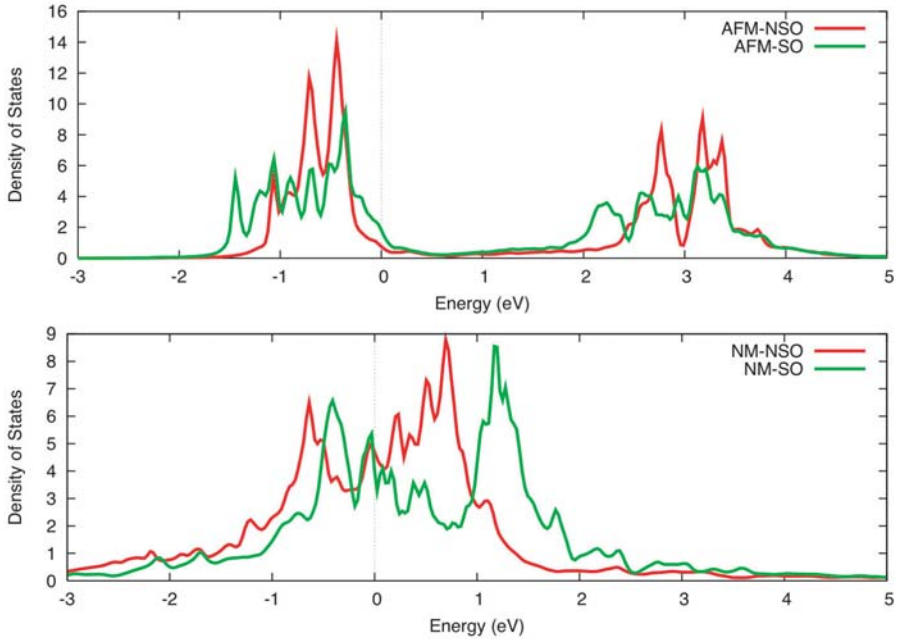

Fig. 7. Density of states of $5f$ electrons in dhcp Am bulk at various theoretical levels. Fermi energy is set at zero.

3.3 5f electron properties of DHCP Am and the (0001) surface

To understand the properties and localization of $5f$ electrons in dhcp Am bulk and the (0001) surface, the density of states (DOS) of $5f$ electrons have been studied. First, we calculated the DOS of $5f$ electrons at each equilibrium lattice constant for dhcp Am bulk at both nonmagnetic and antiferromagnetic state with and without spin-orbit coupling and plotted the results in Figure 7. From the DOS plot in Figure 7, (1) we notice that only at the nonmagnetic state, there is a broad peak across the Fermi level, signifying a large density of states at the Fermi level implying an itinerant band. In sharp contrast to this behavior, at the antiferromagnetic state, there are two well separated peaks on the DOS plot, implying the first peak is associated with the $5f_{5/2}$ sub-shell being almost full and the second peak can be associated with the $5f_{7/2}$ sub-shell being almost empty. Such behaviors of dhcp Am $5f$ electrons are due to its $5f$ electrons localization [14]; (2) at the antiferromagnetic state, as the spin orbit coupling is included the peak before the Fermi level becomes broader and the center further withdraws from the Fermi level. Here the spin-orbit coupling effects might tend to favor the delocalization of $5f$ electrons in dhcp Am bulk. Spin-orbit coupling effect has been found to favor the delocalization of $5f$ electrons in our previous δ-Pu studies [27]. We attribute this to the inherently similar properties of $5f$ electrons in dhcp Am and in δ-Pu and further signals the importance of spin-orbit coupling effects in the electronic structure properties of both bulk Am and Pu; (3) we also notice that the broad peak before Fermi level of our DOS at the AFM-SO level is centered around 1 eV below the Fermi level instead of the 2.8 eV experimentally found in the X-ray and ultraviolet photoemission spectra of bulk dhcp Am [12], although our value is in good agreement with a recently calculated DOS of dhcp Am [14]. This is partly due to the correlation effects which are underestimated in the present calculation given that density functional theory has been used to describe a strongly correlated system like Am.

Second, we studied the localization of $5f$ electrons in dhcp Am (0001) films at the ground state, i.e., AFM-SO level. The density of states of dhcp Am (0001) films at the AFM-SO level with various number of layers ($N = 1, 4, 7$) have been calculated and plotted in Figure 8 respectively. Several features are observed from the figure: (1) the two $5f$ peaks, one before the Fermi level and the other after the Fermi level, that are well separated by a wide gap indicate that the $5f$ electrons are localized, which is also shown in the dhcp Am bulk DOS at the antiferromagnetic state as previously discussed. The gap width is about 2 eV for both our dhcp Am bulk and (0001) surface calculations; (2) the s, p, and $6d$ DOS are much smaller, compared to the $5f$ DOS. For visibility of the DOS plots, we only show $6d$ DOS in Figure 8. In contrast to the two well separated peaks of $5f$ DOS, the $6d$ DOS only has a rather dispersed and broad band across the Fermi level indicating the delocalized nature, though the magnitude is small and may be negligible; (3) as the thickness of the (0001) Am film increases, there are no apparent feature changes in the DOS, meaning the localization of $5f$ electrons in dhcp Am (0001) films is independent of the thickness up to 7 layers.

4 Conclusions

Full potential all electron density-functional calculations with mixed APW+lo/LAPW basis results show that the

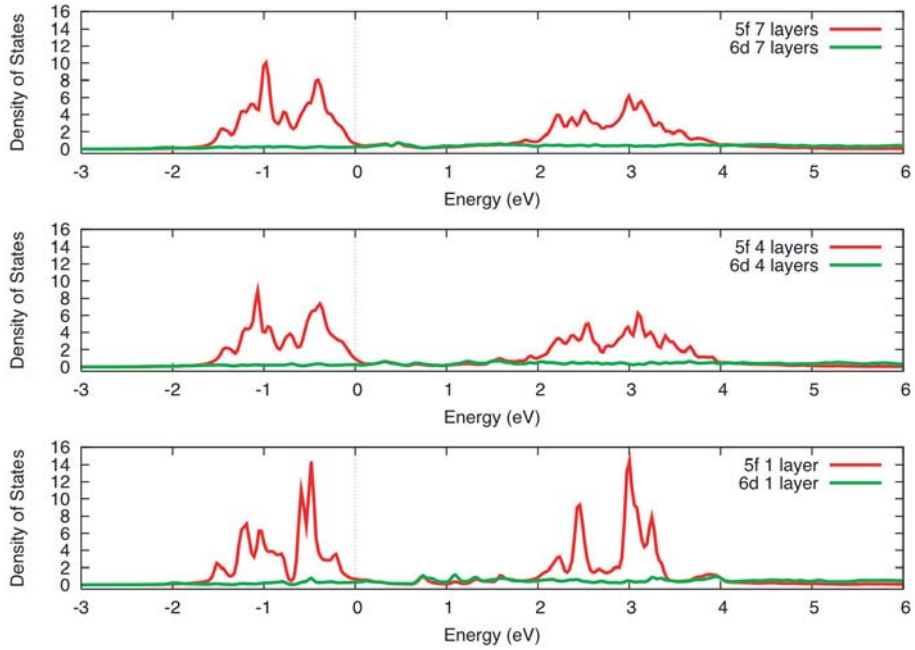

Fig. 8. Density of states of $5f$ and $6d$ electrons for dhcp Am (0001) N-layer slabs at the AFM-SO level, where $N = 1$, 4, 7 as labeled in the figure. Fermi energy is set at zero.

anti-ferromagnetic state with spin-orbit coupling included is the ground state of bulk dhcp Am, with a lattice constant of $a = 6.61$ a.u., a bulk modulus of 27.08 GPa, and a zero magnetic moment, in excellent agreement with experimental observations. Density of states calculations show that $5f$ electrons of dhcp Am bulk are mainly localized at the ground state. The spin-orbit coupling is found to play an important role in determining dhcp Am bulk properties and to increase the delocalization of $5f$ electrons in dhcp Am bulk at the ground state. The ground state of dhcp Am (0001) surface is determined also to be anti-ferromagnetic with spin-orbit coupling included. As the number of layers increases, the total energy of the dhcp Am (0001) surface slab decreases, gradually approaching the bulk value. The surface energy for dhcp Am (0001) semi-infinite surface energy at the ground state is predicted to be 0.84 J/m^2. In addition, the thickness dependence of magnetic moments, work functions, surface energies, cohesive energies, and spin-orbit coupling energies have been studied at various levels of approximations, namely, NM-NSO, NM-SO, AFM-NSO, and AFM-SO. At the AFM-NSO and AFM-SO levels, the magnetic moments show a behavior of oscillation, which becomes smaller with the increase of the number of layers, and gradually the magnetic moments approach the bulk value of zero. Spin-orbit coupling can lower the total energy of dhcp Am (0001) films by ∼7.7 eV/atom at the anti-ferromagnetic and ∼8.7 eV/atom at the nonmagnetic state. The work function of dhcp Am (0001) 7-layer surface at the ground state is predicted to be 2.90 eV. Quantum size effects are found to be more pronounced in work functions than in surface energies.

We appreciate much very useful comments from the referees. This work is supported by the Chemical Sciences, Geosciences and Biosciences Division, Office of Basic Energy Sciences, Office of Science, US Department of Energy (Grant No. DE-FG02-03ER15409) and the Welch Foundation, Houston, Texas (Grant No. Y-1525).

References

1. J.J. Katz, G.T. Seaborg, L.R. Morss, *The Chemistry of the Actinide Elements* (Chapman and Hall, 1986); *Transuranium Elements: A Half Century* edited by L.R. Morss, J. Fuger (American Chemical Society, Washington, D.C., 1992); L.R. Morss, N.M. Edelstein, J. Fuger, *Chemistry of the Actinide and Transactinide, Elements* edited by J.J. Katz, Hon. Ed. (Springer, New York, 2006)
2. *Challenges in Plutonium Science*, Vols. I and II, Los Alamos Science, **26** (2000)
3. R. Haire, S. Heathman, M. Idiri, T. Le Bihan, A. Lindbaum, Nuclear Materials Technology/Los Alamos National Laboratory, 3rd/4th quarter 2003, p. 23
4. *Fifty Years with Transuranium Elements*, Proceedings of the Robert A. Welch Foundation, October 22–23, 1990, Houston, Texas
5. *Actinides 2005 – Basic Science, Applications, and Technology*, Materials Research Society Symposium Proceedings **893** (2006)
6. G.T. Seaborg, W.D. Loveland, *The Elements beyond Uranium* (John Wiley & Sons, Inc. 1990), p. 17
7. S. Heathman, R.G. Haire, T. Le Bihan, A. Lindbaum, K. Litfin, Y. Méresse, H. Libotte, Phys. Rev. Lett. **85**, 2961 (2000)
8. G.H. Lander, J. Fuger, Endeavour **13**, 8 (1989)

9. A.J. Freeman, D.D. Koelling, in *The Actinides: Electronic Structure and Related Properties*, edited by A.J. Freeman, J.B. Darby, Jr (Academic, New York, 1974)
10. B. Johansson, Phys. Rev. B **11**, 2740 (1975)
11. H.L. Skriver, O.K. Andersen, B. Johansson, Phys. Rev. Lett. **41**, 42 (1978)
12. J.R. Naegele, L. Manes, J.C. Spirlet, W. Müller, Phys. Rev. Lett. **52**, 1834 (1984)
13. A. Lindbaum, S. Heathman, K. Litfin, Y. Méresse, Phys. Rev. B **63**, 214101 (2001)
14. M. Pénicaud, J. Phys. Cond. Matt. **14**, 3575 (2002); M. Pénicaud, J. Phys. Cond. Matt. **17**, 257 (2005)
15. S.Y. Savrasov, K. Haule, G. Kotliar, Phys. Rev. Lett. **96**, 036404 (2006)
16. P. Sõderlind, R. Ahuja, O. Eriksson, B. Johansson, J.M. Wills, Phys. Rev. B. **61**, 8119 (2000); P. Sõderlind, A. Landa, Phys. Rev. B. **72**, 024109 (2005)
17. P.G. Huray, S.E. Nave, R.G. Haire, J. Less-Com. Met. **93**, 293 (1983)
18. T. Gouder, P.M. Oppeneer, F. Huber, F. Wastin, J. Rebizant, Phys. Rev. B **72**, 115122 (2005); L.E. Cox, J.W. Ward, R.G. Haire, Phys. Rev. B **45**, 13239 (1992)
19. D. Gao, A.K. Ray, Eur. Phys. J. B **50**, 497 (2006); D. Gao, A.K. Ray, MRS Fall 2005 Symp. Proc. **893**, 39 (2006); D. Gao, A.K. Ray, Surf. Sci. **600**, 4941 (2006)
20. O. Eriksson, J.M. Wills, Phys. Rev. B **45**, 3198 (1992)
21. A.L. Kutepov, S.G. Kutepova, J. Magn. Magn. Mat. **272–276**, e329 (2004)
22. A. Shick, L. Havela, J. Kolorenc, V. Drchal, T. Gouder, P.M. Oppeneer, Phys. Rev. B **73**, 104415 (2006)
23. S.Y. Savrasov, G. Kotliar, E. Abrahams, Nature **410**, 793 (2001); G. Kotliar, D. Vollhardt, Phys. Today **57**, 53 (2004); X. Dai, S.Y. Savrasov, G. Kotliar, A. Migliori, H. Ledbetter, E. Abrahams, Science **300**, 953 (2003); B. Johansson, Phys. Rev. B **11**, 2740 (1975)
24. B. Johansson, A. Rosengren, Phys. Rev. B **11**, 2836 (1975)
25. J.L. Smith, R.G. Haire, Science **200**, 535 (1978)
26. J.C. Griveau, J. Rebizant, G.H. Lander, G. Kotliar, Phys. Rev. Lett. **94**, 097002 (2005)
27. X. Wu, *Density Functional Theory Applied to d- and f- Electron Systems*, Ph.D. Dissertation, The University of Texas at Arlington, 2001; X. Wu, A.K. Ray, Phys. Rev. B **72**, 045115 (2005); A.K. Ray, J.C. Boettger, Phys. Rev. B **70**, 085418 (2004); J.C. Boettger, A.K. Ray, Int. J. Quant. Chem. **105**, 564 (2005); M.N. Huda, *A Relativistic Density Functional Study of The Role of 5f electrons in Atomic and Molecular Adsorptions on Actinide Surfaces*, Ph.D. Dissertation, The University of Texas at Arlington, 2004; M.N. Huda, A.K. Ray, Eur. Phys. J. B **40**, 337 (2004); M.N. Huda, A.K. Ray, Physica B **352**, 5 (2004); M.N. Huda, A.K. Ray, Eur. Phys. J. B **43**, 131 (2005); M.N. Huda, A.K. Ray, Physica B **366**, 95 (2005); M.N. Huda, A.K. Ray, Phys. Rev. B **72**, 085101 (2005); M.N. Huda, A.K. Ray, Int. J. Quant. Chem. **105**, 280 (2005); H.R. Gong, A.K. Ray, Eur. Phys. J. B **48**, 409 (2005); H.R. Gong, A.K. Ray, MRS Fall 2005 Symp. Proc. **893**, 45 (2006); H.R. Gong, A.K. Ray, Surf. Sci. **600**, 2231 (2006)
28. E.K. Schulte, Surf. Sci. **55**, 427 (1976)
29. P.J. Feibelman, Phys. Rev. B **27,** 1991 (1982)
30. E.E. Mola, J.L. Vicente, J. Chem. Phys. **84**, 2876 (1986)
31. I.P. Bartra, S. Ciraci, G.P. Srivastava, J.S. Nelson, C.Y. Fong, Phys. Rev. B **34**, 8246 (1986)
32. J.C. Boettger, S.B. Trickey, Phys. Rev. B **45**, 1363 (1992); J.C. Boettger, Phys. Rev. B **53**, 13133 (1996)
33. C.M. Wei, M.Y. Chou, Phys. Rev. B **66**, 233408 (2002)
34. D.J. Singh, *Plane waves, Pseudopotential and the LAPW Method* (Kluwer, Dordrecht, 1994)
35. E. Stjõstedt, L. Nordstrõm, D.J. Singh, Sol. St. Comm. **114**, 15 (2000)
36. P. Blaha, K. Schwarz, P.I. Sorantin, S.B. Trickey, Comp. Phys. Comm. **59**, 399 (1990); M. Petersen, F. Wagner, L. Hufnagel, M. Scheffler, P. Blaha, K. Schwarz, Comp. Phys. Comm. **126**, 294 (2000); K. Schwarz, P. Blaha, G.K.H. Madsen, Comp. Phys. Comm. **147**, 71 (2002)
37. J.P. Perdew, K. Burke, M. Ernzerhof, Phys. Rev. Lett. **77**, 3865 (1996); J.P. Perdew, K. Burke, Y. Wang, Phys. Rev. B **54**, 16533 (1996); J.P. Perdew in *Electronic Structure of Solids*, edited by Ziesche, H. Eschrig (Akademie Verlag, Berlin, 1991)
38. P. Hohenberg, W. Kohn, Phys. Rev. **136**, B864 (1964); W. Kohn, L.J. Sham, Phys. Rev. **140**, A1133 (1965); *Density Functional Theory for Many Fermion Systems* edited by S.B. Trickey (Academic, San Diego, 1990); R.M. Dreialer, E.K.U. Gross, *Density Functional Theory: An Approach to Quantum Many Body Problem* (Springer, Berlin, 1990); *Electronic Density* Functional *Theory Recent Progress and New Directions*, edited by J.F. Dobson, G. Vignale, M.P. Das (Plenum, New York, 1998)
39. P.E. Blöchl, O. Jepsen, O.K. Andersen, Phys. Rev. B **49**, 16223 (1994)
40. G.K.H. Madsen, P. Blaha, K. Schwarz, E. Sjostedt, L. Nordstrom, Phys. Rev. B **64**, 195134 (2001)
41. D.D. Koelling, B.N. Harmon, J. Phys. C: Sol. St. Phys. **10**, 3107 (1977)
42. A.H. MacDonnald, W.E. Picket, D.D. Koelling, J. Phys. C: Sol. St. Phys. **13**, 2675 (1980)
43. P. Novak, `$WIENROOT/SRC/novak_lecture_on_spinorbit.ps(WIEN2K)`
44. R.W.G. Wyckoff, *Crystal Structures* (Wiley, New York, 1963), Vol. 1
45. F.D. Murnaghan, Proc. Natl. Acad. Sci. USA **30**, 244 (1944)
46. D.M. Teter, G.V. Gibbs, M.B. Boisen, Jr, D.C. Allan, M.P. Teter, Phys. Rev. B **52**, 8064 (1995)
47. J.G. Gay, J.R. Smith, R. Richter, F.J. Arlinghaus, R.H. Wagoner, J. Vac. Sci. Tech. A **2**, 931 (1984)
48. J.C. Boettger, Phys. Rev. B **49**, 16798 (1994)
49. V. Fiorentini, M. Methfessel, J. Phys. Cond. Matt. **8**, 6525 (1996)
50. C.J. Fall, N. Binggeli, A. Baldereschi, J. Phys. Cond. Matt. **11**, 2689 (1999)
51. U. Benedict *Handbook on the Physics and Chemistry of the Actinides*, edited by A.J. Freeman, G.H. Lander (Amsterdam, North-Holland, 1987), Vol. 5